Contents list available at IJRED website

International Journal of Renewable Energy Development

Journal homepage: https://ijred.undip.ac.id

Research Article

Numerical Investigation of a Solar PV/T Air Collector Under the Climatic Conditions of Zarqa, Jordan

Salem Nijmeh[a]*, Ahmad Bani Yaseen[a], Moh'd Sami Ashhab[b], Mohammad Juaidy[a]

[a] *Department of Mechanical Engineering, Faculty of Engineering, The Hashemite University, Zarqa, Jordan.*

[b] *Department of Mechanical Engineering, Al Hussein Technical University, Amman, Jordan.*

Abstract. The use of hybrid photovoltaic/thermal (PV/T) and low concentrating photovoltaic/thermal (LCPV/T) systems can significantly enhance the overall solar energy conversion efficiency by delivering electricity and thermal energy. This paper presents a case study using a standing PV system's theoretical and modeling approach that can be modified to adapt to the hybrid technology. Firstly, a single-pass conventional PV/T air-cooled collector is investigated based on heat transfer and electrical models under the climatic conditions of Zarqa, Jordan. The performance parameters are evaluated using thermal and electrical properties of the considered PV installation and measured meteorological data. Results show that the total energy produced varies between a maximum of 134.6 kWh/m^2 in July and a minimum of 81.7 kWh/m^2 in January. The annual average hourly variation of overall energy efficiency ranges between 79.2% and 88.4%. Moreover, the dissipated thermal energy can meet 63.6% of the total energy required to ventilate the Hashemite University Presidency Building during the winter months. Finally, the performance of the modeled PV/T system air system coupled with flat boosters to provide a low irradiation concentration ratio (CR) is explored. The maximum electric output of the resulting LCPV/T system is compared with the uncooled system. It is found that the percentage improvement due to air cooling ranges between 0.72% at CR=1 and 2.77% at CR=2.5.

Keywords: PV/T air collector, Low concentration ratio, Numerical simulation, Useful thermal energy, Overall energy efficiency.

Received:19th March 2022; Revised: 1st June 2022; Accepted: 22nd June 2022; Available online: 1st July 2022

1. Introduction

Jordan has limited conventional energy resources, and imports of energy form oil products and natural gas account for 94% of the primary energy supply in 2018. The cost of consumed energy represented 10% of GDP in 2018 (Energy 2019). Jordan's energy strategy is centered mainly on expanding the use of natural gas, oil shale, and renewable energy RE, particularly in the electricity production sector. The strategy sets an ambitious target to increase the contribution of RE to 10% in the energy mix (Abu-Rumman *et al.* 2020). To reach this goal, the Renewable Energy and Energy Efficiency Law (REEEL) No.13 was adopted in 2012 as a legislative and structural umbrella for the advancement of RE in Jordan (Energy law No. 13 2012). The law permits Independent Power Producers (IPP) to supply RE-generated power to the National Electric Power Company (NEPCO) according to 20 years Power Purchase Agreement (PPA) (Nijmeh *et al.* 2020). The strategy and subsequent law are bearing fruits, with the contribution of renewable energy to the total electricity generated in 2019 reached 14.9%, of which about 10.4 % by solar energy (Annual Report 2019). The total installed RE power is estimated to reach 2400 MWp by 2021, and that will represent 20% of the overall electricity production. The largest and latest solar PV plant in Jordan is the Masdar Company project, with a 200 MWp capacity (Baynouna 2020). Jordan has huge potential for solar energy utilization as it lies within the solar belt of the world with daily average solar irradiance between 4-8 kWh/m^2, which adds up to a total of 1400-2300 kWh/m^2 annually (Alrwashdeh *et al.* 2018).

Solar systems can be categorized into two technology groups: thermal and photovoltaic. The hybrid photovoltaic /thermal (PV/T) collector system combines the two technologies in one unit and can produce electricity and thermal energy simultaneously (Mustapha *et al.* 2018). The heat output can be utilized in different applications, such as drying, solar cooling, desalination, building, and water heating (Rukman *et al.* 2019). This will result in higher overall efficiency and a reduction in equipment cost and size compared to using separate systems. Another important benefit of the hybrid PV/T system is removing waste heat from the PV module by the cooling medium. This leads to a reduction in the temperature of the PV cell and an enhancement in electrical efficiency. The rising temperature of the PV module causes a reduction in power output which is determined by the temperature coefficient. A simulation study carried out in Amman, Jordan, at various working temperatures shows that the power

* Corresponding author:
Email: drnijmeh@hu.edu.jo (S. Nijmeh)

https://doi.org/10.14710/ijred.2022.45306
ISSN: 2252-4940/© 2022.The Author(s). Published by CBIORE

output of five PV panels decreased between 0.25% and 0.30% for every 1°C rise (Alrwashdeh 2018).

Another undesirable result of high temperatures is faster power degradation. The elevated temperatures and other external effects cause intrinsic property changes in PV materials and defects in interconnections and solder bonds, which lead to accelerated degradation rates and shorter lifespan (Okorieimoh *et al*. 2019). For example, research in India calculated that the average power decline of 90 PV m-Si modules over 22 years is 1.9%/year (Rajput *et al*. 2016). Visual inspection and thermal imaging reveal several defects in cell and string inter-connection ribbon, back-sheet chalking, and other problems.

1.1. Photovoltaic thermal PV/T systems

The PV/T systems can be classified into different types based on the cooling medium: air-based PV/T systems, liquid-based PV/T systems such as water or nanofluids, and a combination of both air and liquid-based system (Fudholi & Sopian 2018). Liquid-based PV/T collectors have higher electrical and thermal efficiencies due to the superior thermal conductivity of the heat transfer medium. However, they are more complex and expensive and can have freezing problems in cold weather. Many studies have been conducted on different types of liquid-based systems over the past few years. For example, experiments were conducted on a PVT system in Zarqa, Jordan, operating under active water-backside cooling (Eteir *et al*. 2021). Tests show an increase in electrical efficiency of 6.9%. Researchers carried out an experimental investigation of cooling PV systems using water and two different types of nanofluids under the climate conditions of Jerash, Jordan (Ebaid *et al*. 2018). The average increase in electrical output for TiO_2 nanofluid and water cooling compared to no cooling is 6.05% and 3.75%, respectively.

On the other hand, PV/T air systems are less efficient than liquid-based ones due to the low thermal conductivity of air. However, they are less complex, more cost-effective, and require little maintenance. The classical type is the conventional or back-pass air-based system shown in Fig. 1.

Over the past decade, many attempts have been made to enhance the performance of the PV/T air system by implementing various designs and modifications. For instance, Slimenai et al. presented a comparative numerical study between PV modules and three different PV/T air collectors under the climatic conditions of Algiers. It is found that the glazed double-pass collector achieved the best results with a daily average overall energy efficiency of 74% (Slimenai *et al*. 2017). Experimental work was conducted in Busan, Korea on a novel PV/T single-pass double-flow air channel collector with a non-uniform cross-section transverse rib attached to the back of the PV module (Choi *et al*. 2020). The maximum electrical and overall thermal efficiencies attained were 14.81% and 71.54%, respectively, at mass the flow rate of 0.07698 kg/s. Mojunder *et al* proposed and tested a single pass PV/T air collector integrated with a thin flat metallic sheet and fins. Results show that the maximum electrical and thermal efficiencies achieved were 14.03% and 56.19%, respectively, for the case of four fins, 0.14 kg/s mass flow rate, and 700 W/m² solar radiation (Mojunder *et al*. 2016). Pauly *et al* proposed and numerically studied a novel PV/T air collector with a variable cross-sectional duct to reduce the temperature gradient over the panel surface.

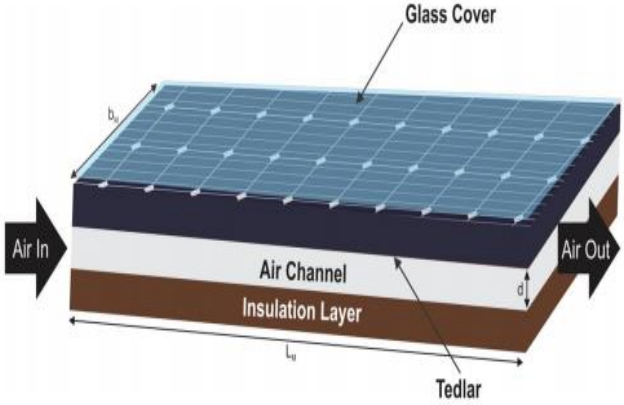

Fig. 1 Layer diagram of conventional PV/T air collector (Diwania *et al*. 2020).

Results show a 20% improvement in overall performance compared to conventional PV/T air collector (Pauly *et al*. 2016). The performance of a double pass PV/T air collector with and without fins was evaluated in another study. The increased surface area due to fins reduced the cell temperature from 82°C to 66°C, which means higher electrical efficiency (Kumar & Rosen 2011). Other methods investigated to improve the efficiency of PV/T systems include using corrugated surfaces, finned absorber with phase change material, and porous media (Fudholi *et al*. 2019). Comprehensive reviews of recent developments, applications, and performance data of air and water PV/T systems are presented in several works (Lamnatou & Chemisana 2017, *Fudholi et al*. 2019).

1.2. Applications of PV/T air collector systems

The thermal output of the PV/T air system can be directly used for drying crops, greenhouse heating, building heating, etc. For example, a numerical study was conducted on the performance of a single-pass PV/T air collector used to preheat the supply air of a tertiary building in Fez, Morocco. The main results show an increase in electrical efficiency by 2% and an annual saving of 38.3% in the heating requirement of the building (Hachchadi *et al*. 2018). Tiwari et al presented thermal modeling of PV/T air collector integrated greenhouse drying system. Simulation results obtained for electrical and thermal efficiencies are 11.26% and 26.68%, respectively, at an air mass flow rate of 0.01 kg/s (Tiwari *et al*. 2018). Another experimental and parametric study on applications of PV/T air systems was conducted in Tunis (Fterich *et al*. 2018). The prototype system was utilized to dry tomatoes. Results show enhancement of electric efficiency, improved drying crop quality, and decrease in drying time compared to sun drying. This hybrid PV/T air system may be well-suited for rural areas in Jordan, where farmers can exploit the hot air to preserve agricultural products such as grapes, apricots, tomatoes, etc., by drying. The electrical energy output can be utilized for lighting, irrigation, water pumping, and refrigerated storage.

1.3. Concentrating photovoltaic thermal CPV/T systems

As mentioned earlier, the conventional PV/T collector combines the technologies of PV and solar thermal systems. However, it delivers low-temperature heat which

has limited applications and relatively small electrical efficiency. The concentrating photovoltaic thermal CPV/T system employs optical parts to enhance solar irradiation and generate significantly higher electrical and thermal outputs than the conventional PV/T system. The medium-grade heat produced can be utilized in various domestic and industrial solar energy applications. The CPV/T systems have an excellent potential to compete with conventional power generation systems in the future (Daneshazarian *et al*. 2018).

The CPV/T systems can be classified into three categories: Low concentration ratio CR (1-10 suns) systems (known as LCPV/T collectors), medium CR (10 – 100 suns) systems (MCPV/T collectors), and high or ultra-high CR (> 100 suns) systems (HCPV/T collectors) (Shanks *et al*. 2016). Simple optical elements such as compound parabolic concentrators (CPC), V-trough concentrators, Fresnel reflectors, and flat planar reflectors or boosters can achieve a low concentration ratio. For low CR, static 2–D plane reflectors are more cost-effective than any other type of optical elements, such as lenses to be applied with fixed PV panels. Ju *et al* conducted a comprehensive review of LCPV/T systems in the literature. The main outcomes are flat-plate reflectors mounted on one or two sides of PV panel, V-trough solar concentrators and CPC optical elements to achieve CR less than 4 (Ju *et al*. 2017). These systems are best installed as fixed; tracking can add an unjustified increase in cost and complexity. Passive cooling is a fine choice for the flat-planar LCPV/T systems, although active cooling is more frequently employed. Finally, all commercially available silicon cells are commonly used in LCPV/T systems.

Over the last decade, several studies have been conducted on LCPV/T and LCPV (without heat recovery capabilities) systems using different optical elements to assess their potential. For example, experiments were carried out on stationery and tracking PV panels with different reflectors (Rizk & Nagiral 2008). The tests incorporated aluminum, stainless steel and, chrome film reflectors. It was found that an increase of 40% in power output was obtained using this concentration method. Al-Najideen et al tested a novel double V-trough solar concentrator (DVSC) with CR greater than three suns. It is found that the PV power increased five folds at a reflector tilt angle of 71° (Al-Najideen *et al*. 2019). Another experimental investigation was recently carried out in India on a mirror integrated PV system (MIPVS). It is concluded that the MIPVS system produces a 30.3% enhancement in yearly energy output compared to the conventional PV system (Odungat *et al.* 2020). Amanlou *et al* investigated theoretically using CFD, an air-cooled LCPV/T system with a new design concave-side walls diffuser. An improvement in electrical, thermal, and overall efficiencies was obtained by 36%, 42.2% and 40.5%, respectively (Amanlou *et al*. 2018).

Many research papers are presented in the literature to investigate the utilization of LCPV/T air and water systems in various applications. For instance, experimental work was performed on a parabolic trough concentrator LCPV/T collector with CR=5.5 for drying honeysuckle flowers. Drying temperature varied between 65 - 80 °C, and the overall efficiency ranged between 50 - 57% (Geng *et al.* 2013). Mansy et al presented a simulation study of water-cooled LCPV/T collector with CR=2 to supply electricity and hot water to a small campus at Mansoura University, Egypt. The results indicate that the electrical efficiency increased significantly, and an annual average cogeneration efficiency of 60.5% was achieved (Mansy et al. 2020). Another recent research work on LCPV/T system utilization in buildings was conducted in Chuncheon, South Korea (Hussain & Kim 2019). The water-glycol cooled hybrid system which employs 8 Fresnel lenses reduced building heating costs significantly in cold winter months (34% in December). Comprehensive reviews of air and water based CPV/T systems are presented in several works (Bandaru *et al*. 2021; Daneshazarian *et al*. 2018; Ju *et al*. 2017). The reviews cover detailed descriptions of various design configurations, performance evaluations, and heat recovery applications. The findings are very encouraging and conclude that CPV/T collectors have the capability to be economically viable in the near future.

The medium and high concentration photovoltaic thermal (MCPV/T and HCPV/T) systems are beyond the scope of this work. They are more sophisticated and expensive than LCPV/T systems. An effective heat rejection means it is necessary to avoid heat damage, boost efficiency and lifespan. Examples of HCPV/T system thermal energy applications include solar absorption cooling (Alobaid et al. 2017) and Organic Rankine Cycle (ORC) for hydrogen production (Hosseini & Butler 2021).

In this work, a conventional PV/T collector system with an air-channel installed at the backside of the PV panel to remove waste heat is adopted and modeled via MATLAB. This type is chosen due to its simplicity and non-invasive nature that could be applied to existing systems at the Hashemite University. Heat transfer and electrical models required to evaluate the system's performance are presented. The meteorological data, including solar irradiation and ambient temperature, are obtained from experimental measurements. The exploitation of dissipation heat to fulfill the ventilation load requirement of the Hashemite University Presidency Building in winter is investigated. The electrical and thermal outputs can be further enhanced by integrating the PV/T collector with optical parts to concentrate the solar irradiation. In our case, we are interested in stationary air-cooled LCPV/T systems with optical elements capable of achieving concentration ratios of less than 3 for their simplicity and low cost. The optical elements such as planar reflectors can be easily manufactured locally without needing advanced technology. The temperature rise is usually not large so, the conventional passive or active air-cooling technique is very satisfactory. This simple air heat dissipation system requires little or no maintenance. Tracking is not required, which lowers the initial and maintenance costs significantly. Moreover, all types of commercially available silicon cells are typically used in LCPV/T systems. This work studies the suitability of passive air cooling and improved electrical output at different concentration ratios.

2. Methodology

This paper presents a case study using a comprehensive theoretical and modeling approach of an existing PV system that can be modified to adapt the PV/T and LCPV/T technology. The model evaluates the cell temperature, the possibility of passive air cooling, and enhancement in generated electrical output at different concentration ratios. No data have been reported in the literature regarding these significant outcomes.

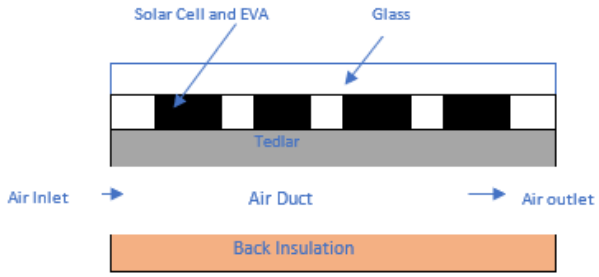

Fig. 2 Cross-sectional view of PV/T air collector.

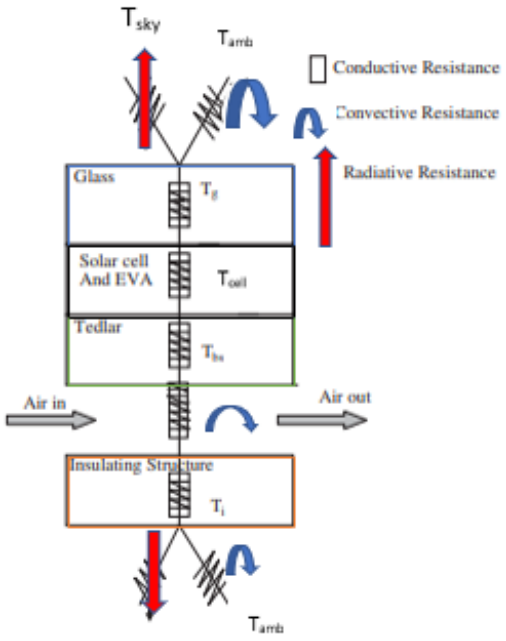

Fig. 3 Equivalent thermal resistance network.

2.1. Photovoltaic/thermal air-cooled model

A cross-sectional view of the adopted PV/T air system model and its corresponding thermal resistance network are shown in Figs. 2 and 3. The design parameters and thermophysical properties of the modeled PV/T air collector system are presented in Table 1. The modeled PV system is mounted on the rooftop of the Presidency Building at the Hashemite University in Zarqa, Jordan (32.1° N, 36.2° E). It is a fixed installation with a tilt angle of 26° and an azimuth angle of zero. The system consists of 28 Poly-Crystalline cell-type modules with a nominal capacity of 285 W (STP285-24/Vd, SunTech), wired in two strings. The total capacity of the system is 7.98 kWp (DC).

2.2. Thermal analysis

The energy balance equations for the various sections of our considered PV/T system are as follows: (Sarhaddi *et al*. 2010; Pauly *et al*. 2016; Tiwari & Sodha 2007; Abdullah *et al*. 2019). For the PV module, the amount of solar energy absorbed after optical losses is the summation of total heat loss from the top surface of the cell to the ambient, the heat loss from the cell to the back surface of Tedlar and the electrical power delivered.

Table 1
Physical, thermal and optical properties of PV/T air collector system.

PV module type	Poly-crystalline Silicon, SUNTECH (STP285-24/Vd)
Dimensions (mm)	1956 x 992 x 50
Duct length (m)	1.95
Duct breadth (m)	0.99
Duct cross sectional area (m^2)	0.04455
Thickness of silicon solar cell (m)	0.0003
Conductivity of silicon solar cell (W/m.K)	0.036
Thickness of Tedlar (m)	0.0005
Conductivity of Tedlar (W/m.K)	0.033
Thickness of solar glass cover (m)	0.004
Conductivity glass cover (W/m.K)	1
Thickness of back insulation (m)	0.05
Conductivity of back insulation (W/m.K)	0.035
Transmissivity of glass cover	0.95
Absorptivity of solar cell	0.85
Packing factor of solar cell	0.745
Absorptivity of Tedlar	0.5
Convective heat transfer coefficient in the air duct ($W/m^2.K$)	30
The product of effective absorptivity and transmissivity	0.619

This can be translated by eq (1):

$$\tau_g[\alpha_c\beta_c + \alpha_T(1-\beta_c)]Gbdx = [U_t(T_{cell} - T_{amb}) + U_T(T_{cell} - T_{bs})]bdx + \eta_{el}\tau_g\beta_c Gbdx \quad (1)$$

Where T_{amb}, T_{cell}, T_{bs}, G, b, dx, α_c, α_T, β_c, τ_g, and η_{el} are the ambient air temperature, solar cell temperature, back surface temperature of Tedlar, incident solar irradiation, width of air collector, elemental length duct, absorptivity of solar cell, absorptivity of Tedlar, packing factor of solar cell, transmittance of glass, and PV cell electrical efficiency, respectively. Moreover, U_T is the conductive heat transfer coefficient from solar cell to passing air through Tedlar.

Energy balance for the back surface of Tedlar, is given by Eq (2):

$$U_T(T_{cell} - T_{bs})bdx = h_f(T_{bs} - T_{air})bdx \quad (2)$$

Where T_{air} and h_f are the air temperature in channel and the convective heat transfer coefficient, respectively.
Finally, the energy balance for passing fluid through the channel is follows in Eq (3):

$$\dot{m}_a C_p\left(\frac{dT_{air}}{dx}\right)dx + U_b(T_{air} - T_{amb})bdx = h_f(T_{bs} - T_{air})bdx \quad (3)$$

Where $\dot{m}_a$ and C_p are the mass flow rate and specific heat capacity of air. Also, U_b is the bottom heat transfer coefficient from air stream to the ambient.
The mass flow rate $\dot{m}_a$ is given by Eq (4):

$$\dot{m}_a = \rho_a V_{in} A_d \quad (4)$$

Where, ρ_a, V_{in}, A_d are the air density, inlet velocity, and cross-sectional area of channel, respectively. The mass flow rate is 0.147 kg/s at inlet velocity of 3 m/s which is equal to the average annual wind velocity for the location.

The heat balance equations can be solved to derive expressions for the key thermal parameters of the

proposed PV/T air collector. The outlet air temperature $T_{air,\ out}$, average air temperature $\bar{T}_{air}$, back surface temperature T_{bs}, and solar cell temperature T_{cell} are given by (Das *et al*. 2018; Slimani *et al*. 2017; Abdullah *et al*. 2019; Sarhaddi *et al*.2010):

$$T_{air,out} = \left[\frac{P_1P_2(\tau\alpha)_{eff}G}{U_L} + T_{amb}\right]\left(1 - e^{(-bU_L/\dot{m}_a C_a)L}\right) + T_{air,in}e^{(-bU_L/\dot{m}_a C_a)L} \quad (5)$$

$$\bar{T}_{air} = \left[\frac{P_1P_2(\tau\alpha)_{eff}G}{U_L} + T_{amb}\right]\left(1 - \frac{1 - e^{(-bU_L/\dot{m}_a C_a)L}}{bU_L/\dot{m}_a C_a}\right) + T_{air,in}\frac{1 - e^{(-bU_L/\dot{m}_a C_a)L}}{bU_L/\dot{m}_a C_a} \quad (6)$$

$$T_{bs} = \frac{P_1(\tau\alpha)_{eff}G + U_{tT}T_{amb} + h_f\bar{T}_{air}}{U_{tT} + h_f} \quad (7)$$

$$T_{cell} = \frac{(\tau\alpha)_{eff}G + U_tT_{amb} + U_TT_{bs}}{U_t + U_T} \quad (8)$$

The relevant heat loss coefficients in equations (5-8) based are expressed in Eqs (9-11):
The conductive heat transfer coefficient from PV cell to passing fluid U_T. It is expressed in Eq (9):

$$U_T = \left[\frac{X_c}{K_c} + \frac{X_d}{K_d}\right]^{-1} \quad (9)$$

Where X_c, K_c, X_d, and K_d are the thickness of cell, thermal conductivity of cell, thickness of Tedlar, and thermal conductivity of Tedlar, respectively.

The overall heat transfer coefficient at the bottom from passing air to the ambient U_b. It is expressed in Eq (10):

$$U_b = \left[\frac{X_{ins.}}{K_{ins.}} + \frac{1}{h_{c,b}}\right]^{-1} \quad (10)$$

Where $X_{ins.}$, $K_{ins.}$ and $h_{c,b}$ are the thickness of rear insulator, thermal conductivity of rear insulator and convective heat transfer coefficient at the bottom of the solar device, respectively.

The overall top heat loss coefficient to the ambient U_t, incorporates conductive, convective, and radiative modes of heat transfer. It is expressed in Eq (11):

$$U_t = \left[\frac{X_g}{K_g} + \frac{1}{h_{w,v}} + \frac{1}{h_r}\right]^{-1} \quad (11)$$

The radiative heat transfer coefficient is defined by Eq (12):

$$h_r = \varepsilon_g\sigma(T_s + T_{cell})({T_s}^2 + {T_{cell}}^2) \quad (12)$$

The equivalent temperature of the sky is determined by the following simple correlation Eq (13):

$$T_s = 0.0552{T_a}^{1.5} \quad (13)$$

The wind convective heat transfer coefficient is described by the following equation Eq (14):

$$h_{w,v} = 5.7 + 2.8V_w \quad (14)$$

Where X_g, K_g *and* ε_g are the thickness, thermal conductivity, and emissivity of glass cover, respectively, σ is the Stefan-Boltzmann constant, *and* V_w is the wind velocity.

The overall heat transfer coefficient from glass to Tedlar layer through PV cell U_{tT}. It is expressed in Eq (15):

$$U_{tT} = \frac{U_tU_T}{U_T + U_t} \quad (15)$$

The overall heat transfer coefficient from glass to air through PV cell and Tedlar layer U_{tf}. It is expressed in Eq (16):

$$U_{tf} = \frac{U_{tT}h_f}{U_{tT} + h_f} \quad (16)$$

Finally, the overall heat transfer coefficient from the PV/T device to the atmosphere U_L is obtained from Eq (17):

$$U_L = U_b + U_{tf} \quad (17)$$

Additional thermal, optical and parameters presented in equations (5-8) are expressed in Eqs (18-20):

A thermal penalty coefficient due to the existence of PV cell layer, cover and EVA (Ethylene Vinyl Acetate adhesive) is defined in Eq (18):

$$P_1 = \frac{U_T}{U_T + U_t} \quad (18)$$

A thermal penalty coefficient due to the boundary between Tedlar layer and air is definedin Eq (19):

$$P_2 = \frac{h_f}{U_{tT} + h_f} \quad (19)$$

The effective product of absorptance and transmittance is defined in Eq (20):

$$(\tau\alpha)_{eff} = \tau_g[\alpha_c\beta_c + \alpha_T(1 - \beta_c) - \beta_c\eta_{el}] \quad (20)$$

The uncooled working cell temperature $T_{c,uncooled}$ can be computed accurately using Ross simplified linear thermal model as follows in Eq (21) (Bayrakci *et al*. 2014; Schwingshackl *et al*. 2013; Umoette *et al*. 2016):

$$T_{c,uncooled} = T_{amb} + \frac{(NOCT - 20)G}{800} \quad (21)$$

The Nominal Operating Cell Temperature (NOCT) is defined as the cell temperature reached in free standing PV modules under open-circuit under the following conditions: ambient temperature T_{amb}= 20 °C, solar irradiance G= 800 W/m^2 and wind speed 1 m/s. The NOCT has a normal value of 45°C (Suntech 2011).

In this work, the reference module temperature is determined based on Skopali's advanced model expressed in Eq (22) (Idzkowski *et al*. 2020):

$$T_{cell,uncooled} = T_{amb} + \frac{(NOCT - 20)G}{800}.\frac{h_{w,NOCT}}{h_{w,v}}\left[1 - \frac{\eta_{ref}}{\tau\alpha}(1 - \beta_{tc}T_{ref})\right] \quad (22)$$

This enhanced model considers the wind speed whereas the original NOCT model is based on wind speed of 1 m/s. Furthermore, it contains additional cell characteristics such as η_{ref}, β_{tc} and τα.

The product of transmittance of cover system and absorptance of cell (τα) is assumed as 0.9 (Idzkowski *et al*.

2020; Umoette *et al*. 2016). Also, $h_{w,NOCT}$ is the wind convection coefficient at NOCT wind speed (1 m/s) and $h_{w,v}$ is the wind convective heat transfer at speed V_w close to the module.

2.3. Electrical and thermal performance

The most common expression for calculating the PV cell electrical conversion efficiency is based on the following linear correlation Eq (23) (Pauly *et al*. 2016):

$$\eta_{mp} = \eta_{ref}\left[1 + \beta_{tc}\left(T_{cell} - T_{ref}\right)\right] \quad (23)$$

Where η_{mp} is the efficiency of the PV module at its maximum power point, η_{ref} is the efficiency at maximum power point and has a value of 0.147 obtained from manufacturer's data sheets (Suntech 2011). This is under Standard Test Conditions STC: solar irradiance of 1000 W/m^2, reference cell temperature T_{ref} of 25 °C, and air mass 1.5 (Jatoi *et. al.* 2018). Finally, β_{tc} is the temperature coefficient of maximum power with a value of -0.0044 /°C.

The actual maximum power generated by the PV module is defined as follows in Eq (24):

$$P_{mpp} = \eta_{mp}\, A_m G \quad (24)$$

Where A_m is the PV module area (m^2) and G is the incident solar irradiation (W/m^2).

The rate of useful thermal energy obtained from the PV/T air collector can be determined as follows in Eq (25):

$$\dot{Q}_u = \dot{m}_a\, C_p(T_{air,in} - T_{air,out}) \quad (25)$$

The thermal efficiency is the ratio of the useful heat gain of air to the overall incident solar irradiation. It can be computed as (Slimani *et al*. 2017; Abdullah *et al*.2019) in Eq (26):

$$\eta_{th} = \frac{P_{mpp}}{AG} \quad (26)$$

Finally, the overall energy efficiency of the PV/T air collector can be computed by adding the thermal efficiency and thermal equivalent of electrical efficiency (Tiwari & Sodha 2007; Sarhaddi *et al*. 2010) in Eq (27):

$$\eta_{ov} = \eta_{th} + \eta_{th,PV} \quad (27)$$

The conventional electrical efficiency is converted to thermal energy equivalent to compensate the high-grade electrical energy to equivalent low-grade thermal energy using the following relation Eq (28):

$$\eta_{th,PV} = \frac{\eta_{mp}}{C_f} \quad (28)$$

Where C_f is the conversion factor of the thermal power plant and its value is assumed as 0.40 in this work (Tiwari and Sodha 2007; Abdullah *et al*. 2019).
Therefore,

$$\eta_{ov} = \eta_{th} + \frac{\eta_{mp}}{0.40} \quad (29)$$

3. Results and Discussion

3.1. Weather Measurements

The solar irradiance on the 26° tilted plane and ambient temperature measurements were recorded over a one-year testing period. They were analyzed to determine the hourly solar irradiation and ambient temperature for a one-year period. These measured hourly climatic data for the Hashemite University are used as the input data of the numerical simulation conducted using MATLAB. The hourly irradiation values are summed to obtain the daily solar irradiation. The peak value of 7.84 kWh/m^2 is reached on the 1st of July, while the minimum value of 0.87 kWh/m^2 is captured on the 25th of January. The annual average daily irradiation is about 6.15 kWh/m^2. The daily values are added up to obtain the monthly irradiation illustrated in Fig. 4. The maximum and minimum values received are 223.6 kWh/m^2 and 130.8 kWh/m^2 in July and January, respectively. The total annual irradiation is the sum of the monthly values, which is about 2246 kWh/m^2. Our total measured value agrees with a simulation study conducted at the Hashemite University (Etier *et al*. 2010) which reports a total of 2230 kWh/m^2 at an inclination angle of 30°.

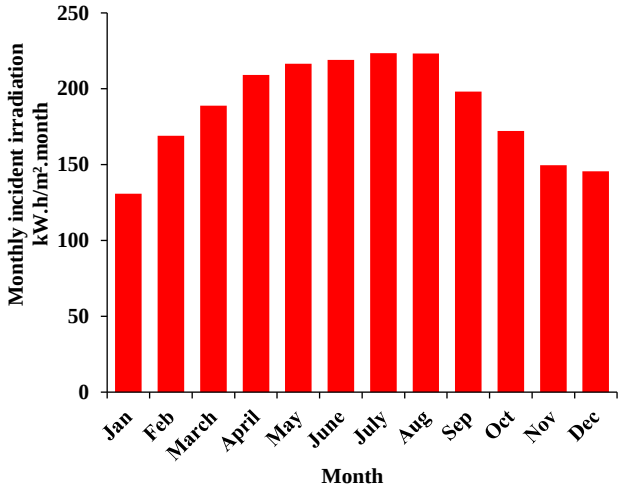

Fig. 4 Monthly incident irradiation on a 26° tilted plane.

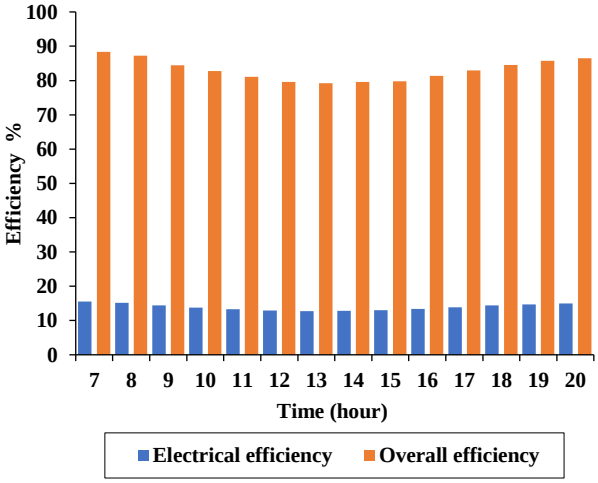

Fig 5 Annual average hourly electrical efficiency and overall energy efficiency.

3.2. Performance analysis of PV/T air system

The annual average hourly variations of electrical efficiency and overall energy efficiency of the hybrid PV/T collector with no concentration are shown in Fig. 5. It can be seen that the electrical efficiency values range between a minimum of 12.71% at 1 PM and a maximum of 15.51% at 7 AM. The hourly averages of overall efficiency vary between 79.2% and 88.4%. These values are consistent with efficiencies reported in the literature. For example, a study conducted in Iraq (Amori & Abd-AlRaheem 2014) on a single duct, single-pass solar PV/T air collector reveals the electrical, thermal, and overall efficiencies at 12 PM reach 8.4%, 53%, and 74%, respectively. The low electrical efficiency is due to the soaring ambient temperatures. An energy review of air-based PV/T collectors found that the overall energy efficiency ranges from 31% to 94% (Fudholi *et al*. 2019). Another comprehensive study (Diwania *et al*. 2020) reports from different references that the thermal efficiency of PV/T air collectors varies from 40% to a maximum of 87%.

The monthly thermal, electrical, and total energy values are evaluated for the PV/T system and the results are shown in Fig. 6. It can be observed that the total energy varies between a maximum of 134.6 kWh/m^2 in July and a minimum of 81.7 kWh/m^2 in January. This is predicted due to the large variation in solar irradiation, ambient temperature, and no of clear days between these two months.

The exploitation of thermal waste heat in preheating the incoming ventilating air supplied to the presidency building during the winter months is investigated. The building with a total area of 1400 m^2 requires 3500 m^3/h of fresh outside air approximately. The monthly variation of thermal gain and ventilation load during the heating season is shown in Fig.7. It can be seen that the thermal gain exceeds the ventilation load requirement in November, February, and March. The excess heat can be further utilized in domestic water and space heating. Furthermore, the percentage contribution of the thermal gain during the coldest months of December and January is equal to 61.3% and 49.9%, respectively. Our proposed system produces 500 kWh/m^2 approximately of thermal energy during the heating season. This is comparable to a conventional PV/T air collector used to heat ventilation air in Fez, Morocco **(**Hachchadi *et al.* 2018), which generates 632.3 kWh/m^2 during the same period. The larger output is due to higher irradiation levels and the utilization of forced air-cooling.

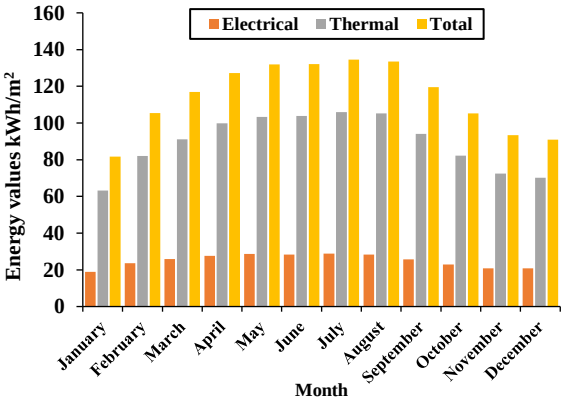

Fig. 6 Monthly thermal, electrical, and total energy values of the PV/T collector.

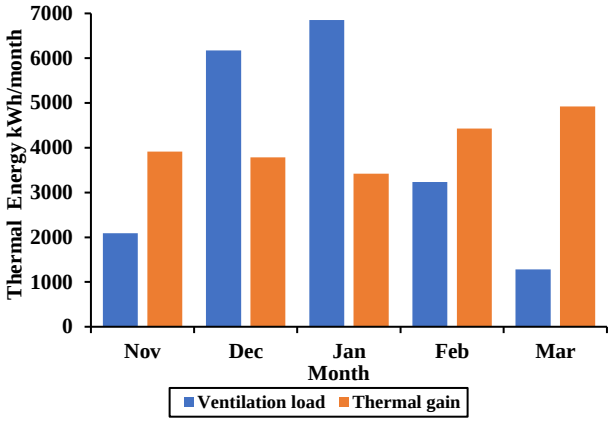

Fig. 7 Monthly variation of thermal gain and ventilation load during the heating season.

3.3. Performance analysis of LCPV/T air system

As for the LCPV/T air-cooled system, the average hourly cell temperature values are evaluated at different concentration ratios (CR's) in August during which the highest values are attained as shown in Fig. 8. The average hourly incident radiation and ambient temperature are also presented. It can be noted that the maximum cell temperature touches 68°C at 1 PM for the case CR=1 (no concentration). This is in broad agreement with experimental measurements for conventional PV/T air systems for summer months in Iraq (Amori & Abd-AlRaheem 2014), with a maximum temperature of 75 °C at 1 PM. The cell temperature rises with a higher CR ratio due to increasing irradiation levels, with a peak temperature of 108.2 °C at CR=2.5. It is evident that concentration ratios higher than 1.5 will result in cell temperatures exceeding the maximum permissible operating temperature of 85 °C. The hourly variation of air-cooled cell temperature is compared with the uncooled one in August at concentration ratios of 1 and 2.5 is presented, as shown in Fig. 9. It can be seen from the figure (9) that the PV cell temperatures considerably decrease when cooling the PV cell.

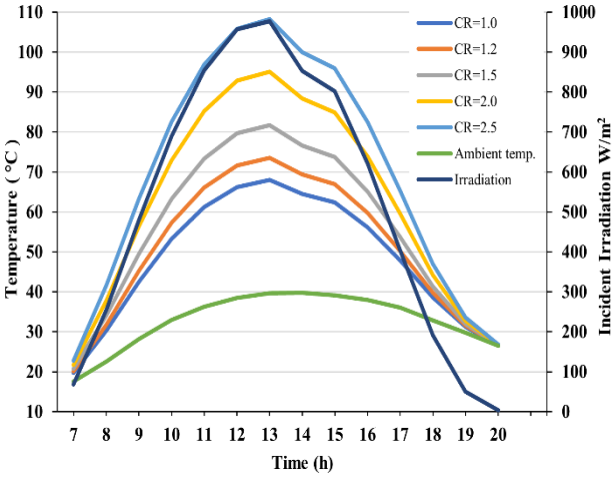

Fig. 8 The hourly variation of incident irradiation, ambient temperature, and cell temperature at different concentration ratios (CR) in August.

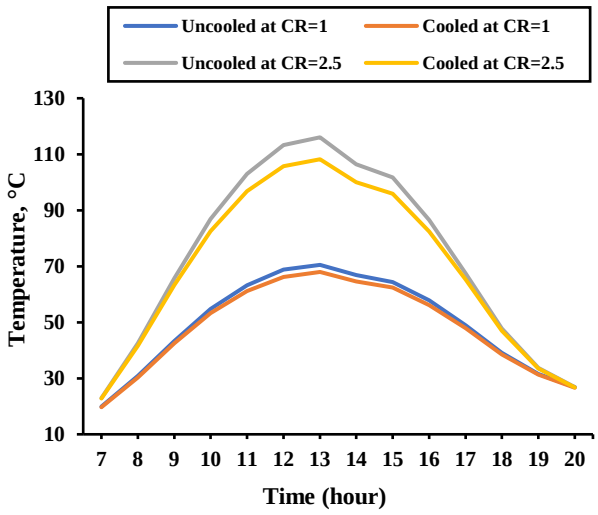

Fig. 9 Comparison of cooled and uncooled cell temperatures in August.

The actual maximum electric power produced by the PV modules is determined and is used to obtain the daily and monthly yield power values in kWh. These calculations are repeated at different concentration ratios to compare the air-cooled CPV/T and uncooled CPV systems.

The resulting percentage improvement in electrical power output due to air-cooling with no concentration for August (Summer), December (Winter), and all-year-round are 1.04%, 0.048%, and 0.72%, respectively, as shown in Fig. 10. This is comparable to a 0.66% increase in predicted annual electrical energy output obtained for a conventional PV/T single pass air collector in Algiers (Slimenai *et al.* 2017). Another study on a similar system in Morocco (Hachchadi *et al.* 2018**)** reveals an average increase of 2%. The larger enhancement is due to the employment of active air-cooling. The effect of air cooling is more pronounced at higher concentration ratios due to the elevated panel temperatures. For example, the corresponding enhancement values at CR=2.5 are 4.24%, 1.68%, and 2.77%, respectively, as shown in Fig. 10.

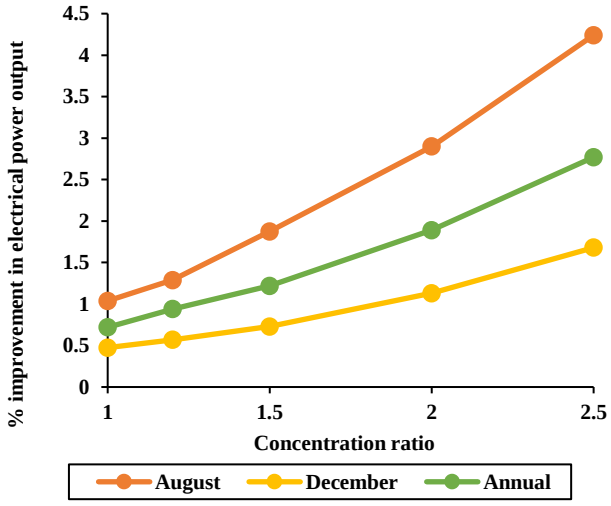

Fig. 10 Percentage improvement in electrical power output at different concentration ratios.

4. Conclusion

In this paper, a case study of a standing PV installation that can be amended to implement the PV/T and LCPV/T technology was performed. A simulation was conducted using thermal-electrical models of the adopted configuration under the climatic conditions of Zarqa, Jordan. Results show that the total energy delivered varies between a maximum of 134.6 kWh/m² in July and a minimum of 81.7 kWh/m² in January, and the annual average overall energy efficiency is 81.6%. In addition, the extracted thermal energy can be exploited to reduce the ventilation heating load of the Hashemite University Presidency Building during December and January by 61.3% and 49.9%, respectively.

Moreover, results reveal that air-cooling of the LCPV/T system leads to all-year-round enhancement in electrical energy output by 0.72% and 2.77% at a concentration ratio CR of 1 and 2.5, respectively. This increase can reach 1.04% and 4.24% in August. However, CR higher than 1.5 will result in cell temperatures exceeding the allowable operating temperature of 85°C. This indicates that passive air cooling is unsuitable above this value.

In order to validate the results of our numerical simulation, experimental research will be conducted in the near future. Additionally, more work will be carried out on the optimum design of the air duct and optical elements of the LCPV/T system.

Nomenclature

Symbols	
A_d	Cross-sectional area of channel (m²)
A_m	PV module area (m²)
b	Width of air collector (m)
C_p	Specific heat capacity of air (J/kg.K)
dx	The elemental length duct (m)
G	Incident solar irradiation (W/m²)
$h_{c,b}$	Convective heat transfer coefficient at the bottom (W/m².K)
h_f	Convective heat transfer coefficient in the air duct (W/m².K)
h_r	Radiative heat transfer coefficient (W/m².K)
$h_{w,NOCT}$	Wind convection coefficient at NOCT wind speed (W/m².K)
K_c	Thermal conductivity of cell (W/m.K)
K_d	Thermal conductivity of Tedlar (W/m.K)
K_g	Thermal conductivity of glass (W/m.K)
K_g	Thermal conductivity glass cover (W/m.K)
K_i	Thermal conductivity of back insulation (W/m.K)
K_{ins}	Thermal conductivity of rear insulator (W/m.K)
K_{si}	Thermal conductivity of silicon solar cell (W/m K)
L	Duct length (m)
L_g	Thickness of solar glass cover (m)
L_i	Thickness of back insulation (m)
L_{si}	Thickness of silicon solar cell (m)
L_T	Thickness of Tedlar (m)
$\dot{m}_a$	Mass flow rate of air (kg/s)
P	Thermal penalty coefficient
P_{mpp}	Actual maximum power generated by the PV module (W)
$\dot{Q}_u$	Rate of useful thermal energy (W)
T_{air}	Air temperature in channel (°C)
$T_{air,\ out}$	Outlet air temperature (°C)
T_{amb}	Ambient air temperature (°C)
T_{bs}	Back surface temperature of Tedlar (°C)
$T_{c,uncooled}$	Uncooled working cell temperature (°C)
T_{cell}	Solar cell temperature (°C)
T_s	Equivalent temperature of the sky (°C)
$\overline{T}_{air}$	Average air temperature (°C)

U_b	Overall heat transfer coefficient at the bottom from passing air to the ambient (W/m².K)
U_L	Overall heat transfer coefficient from the PV/T device to the atmosphere (W/m².K)
U_t	Overall top heat loss coefficient to the ambient (W/m².K)
U_T	Conductive heat transfer coefficient from solar cell to passing air through Tedlar (W/m².K)
U_{tf}	Overall heat transfer coefficient from glass to air through PV cell and Tedlar (W/m².K)
U_{tT}	Overall heat transfer coefficient from glass to Tedlar layer through PV cell (W/m².K)
V_{in}	Inlet velocity (m/s)
V_w	Wind velocity (m/s)
X_c	Thickness of cell (m)
X_d	Thickness of Tedlar (m)
X_g	Thickness of glass (m)
X_{ins}	Thickness of rear insulator (m)

Greek

η_{mp}	Electrical efficiency of the PV module at its maximum power point
η_{ov}	Overall energy efficiency of the PV/T air collector
η_{th}	Thermal efficiency of the PV/T air collector
α_c	Absorptivity of solar cell
α_T	Absorptivity of Tedlar
β_c	Packing factor of solar cell
ϵ_g	Emissivity of glass
η_{el}	PV cell electrical efficiency
ρ_a	Air density (kg/m³)
σ	Stefan-Boltzmann constant (W/m².K⁴)
τ_g	Transmittance of glass cover

References

Abdullah, A. L., Misha, S., Tamaldin, N., Rosli, M. A. M., & Sachit, F. A. (2019). Numerical analysis of solar hybrid photovoltaic thermal air collector simulation by ANSYS. *CFD Letters*, *11*(2), 1-11.

Abu-Rumman, G., Khdair, A., & Khdair, S. (2020). Current status and future investment potential in renewable energy in Jordan: An overview. *Heliyon*, *6*(2), e03346. DOI: 10.1016/j.heliyon.2020.e03346.

Ahmed, A., Shanks, K., Sundaram, S., & Mallick, T. K. (2020). Theoretical investigation of the temperature limits of an actively cooled high concentration photovoltaic system. *Energies*, *13*(8), 1902. DOI: 10.3390/en13081902

Ahmed, O. K., & Bawa, S. M. (2019). The combined effect of nanofluid and reflective mirrors on the performance of photovoltaic/thermal solar collector. *Thermal Science*, *23*(2 Part A), 573-587. DOI: 10.2298/TSCI171203092A

Al-Najideen, M., Al-Shidhani, M., & Min, G. (2019, August). Optimum design of V-trough solar concentrator for photovoltaic applications. In *AIP Conference Proceedings* (Vol. 2149, No. 1, p. 030001). AIP Publishing LLC. DOI: 10.1063/1.5124178

Alobaid, M., Hughes, B., Calautit, J. K., O'Connor, D., & Heyes, A. (2017). A review of solar driven absorption cooling with photovoltaic thermal systems. *Renewable and sustainable energy reviews*, *76*, 728-742. DOI: 10.1016/j.rser.2017.03.081

Alrwashdeh, S. S. (2018). Comparison among solar panel arrays production with different operating temperatures in Amman-Jordan. *International Journal of Mechanical Engineering and Technology*, *9*(6), 420-429.

Alrwashdeh, S., Alsaraireh F., & Saraireh M. (2018). Solar radiation map of Jordan governorates. *International Journal of Engineering & Technology*, *7*(3), 1664-1667. DOI: 10.14419/ijet.v7i3.15557

Amanlou, Y., Hashjin, T. T., Ghobadian, B., & Najafi, E. G. (2018). Air cooling low concentrated photovoltaic/thermal (LCPV/T) solar collector to approach uniform temperature distribution on the PV plate. *Applied Thermal Engineering*, *141*, 413-421. DOI: 10.1016/j.applthermaleng.2018.05.070

Amori, K. E., & Abd-AlRaheem, M. A. (2014). Field study of various air based photovoltaic/thermal hybrid solar collectors. *Renewable Energy*, *63*, 402-414. DOI: 10.1016/j.renene.2013.09.047

Annual Report 2018 (2019). National Electric Power Company (NEPCO). Amman, Jordan.

Bandaru, S. H., Becerra, V., Khanna, S., Radulovic, J., Hutchinson, D., & Khusainov, R. (2021). A Review of Photovoltaic Thermal (PVT) technology for residential applications: performance indicators, progress, and opportunities. *Energies*, *14*(13), 3853. DOI: 10.3390/en14133853

Baynouna Solar Energy Project-Factsheet (2020). Masdar Company.

Bayrakci, M., Choi, Y., & Brownson, J. R. (2014). Temperature dependent power modeling of photovoltaics. *Energy Procedia*, *57*, 745-754. DOI: 10.1016/j.egypro.2014.10.282

Choi, H. U., & Choi, K. H. (2020). Performance evaluation of PV/T air collector having a single-pass double-flow air channel and non-uniform cross-section transverse rib. *Energies*, *13*(9), 2203. DOI: 10.3390/en13092203

Daneshazarian, R., Cuce, E., Cuce, P. M., & Sher, F. (2018). Concentrating photovoltaic thermal (CPVT) collectors and systems: Theory, performance assessment and applications. *Renewable and Sustainable Energy Reviews*, *81*, 473-492. DOI: 10.1016/j.rser.2017.08.013

Das B, Rezaie B, Jha P, Gupta R. (2018). Performance Analysis of Single Glazed Solar PVT Air Collector in the Climatic Condition of NE India. *Proceedings*. 2(4), 171. DOI: 10.3390/ecea-4-05021

Diwania, S., Agrawal, S., Siddiqui, A. S., & Singh, S. (2020). Photovoltaic–thermal (PV/T) technology: a comprehensive review on applications and its advancement. *International Journal of Energy and Environmental Engineering*, *11*(1), 33-54. DOI: 10.1007/s40095-019-00327-y

Ebaid, M. S., Ghrair, A. M., & Al-Busoul, M. (2018). Experimental investigation of cooling photovoltaic (PV) panels using (TiO2) nanofluid in water-polyethylene glycol mixture and (Al2O3) nanofluid in water-cetyltrimethylammonium bromide mixture. *Energy Conversion and Management*, *155*, 324-343. DOI: 10.1016/j.enconman.2017.10.074

Energy (2019) *Facts and Figures brochure*; Ministry of Energy and Mineral Resources. Amman, Jordan.

Etier, I., Al Tarabsheh, A., & Ababne, M. (2010). Analysis of solar radiation in Jordan. *Jordan J Mech Ind Eng*, 4(6), 733-737.

Etier, I., Nijmeh, S., Shdiefat, M., & Al-Obaidy, O. (2021). Experimentally evaluating electrical outputs of a PV-T system in Jordan. *International Journal of Power Electronics and Drive Systems*, *12*(1), 421. DOI: 10.11591/ijpeds.v12.i1.pp421-430

Fterich, M., Chouikhi, H., Bentaher, H., & Maalej, A. (2018). Experimental parametric study of a mixed-mode forced convection solar dryer equipped with a PV/T air collector. *Solar Energy*, *171*, 751-760. DOI: 10.1016/j.solener.2018.06.051

Fudholi, A., & Sopian, K. (2018). R&D of Photovoltaic Thermal (PVT) Systems: an overview. *International Journal of Power Electronics and Drive Systems*, *9*(2), 803. DOI: 10.11591/ijpeds.v9.i2.pp803-810

Fudholi, A., Musthafa, M.F., Ridwan, A., Yendra, R., Desvina, A.P., Rahmadeni, R., Suyono, T. and Sopian, K. (2019). Energy and exergy analysis of air based photovoltaic thermal (PVT) collector: a review. *International Journal of Electrical and Computer Engineering*, *9*(1), 109. DOI: 10.11591/ijece.v9i1.pp109-117

Fudholi, A., Zohri, M., Taslim, I., Aliyah, F., & Koto, A. G. (2019). Heat transfer and efficiency of dual channel PVT air collector: a review. *International Journal of Power Electronics and Drive Systems*, *10*(4), 2037. DOI: 10.11591/ijpeds.v10.i4.pp2037-2045

Geng, W. G., Gao, L., Ma, X. X., Ma, X. L., Yu, Z. Y., & Li, X. Y. (2013). Honeysuckle Drying by Using Hybrid ConcentratorPhotovoltaic-Thermal (PV/T) Dryer: An Experimental Study. In *Applied Mechanics and Materials* (Vol. 291, pp. 132-136). Trans Tech Publications Ltd. DOI: 10.4028/www.scientific.net/AMM.291-294.132

Hachchadi, O., Bououd, M., & Mechaqrane, A. (2018, December). Numerical investigation of a solar PVT air collector used for preheating the ventilating air in tertiary building under the climatic conditions of Fez, Morocco. In *AIP Conference Proceedings* (Vol. 2056, No. 1, p. 020022). AIP Publishing LLC. DOI: 10.1063/1.5084995

Hosseini, S. E., & Butler, B. (2021). Design and analysis of a hybrid concentrated photovoltaic thermal system integrated with an organic Rankine cycle for hydrogen production. *Journal of Thermal Analysis and Calorimetry*, *144*(3), 763-778. DOI: 10.1007/s10973-020-09556-4

Hussain, M. I., & Kim, J. T. (2019). Energy and economic potential of a concentrated photovoltaic/thermal (CPV/T) system for buildings in South Korea. *Journal of Asian Architecture and Building Engineering*, *18*(2), 139-144. DOI: 10.1080/13467581.2019.1606718

Idzkowski, A., Karasowska, K., & Walendziuk, W. (2020). Temperature Analysis of the Stand-Alone and Building Integrated Photovoltaic Systems Based on Simulation and Measurement Data. *Energies*, *13*(16), 4274. DOI: 10.3390/en13164274

Jatoi, A. R., Samo, S. R., & Jakhrani, A. Q. (2018). Influence of temperature on electrical characteristics of different photovoltaic module technologies. *International Journal of Renewable Energy Development*, *7*(2), 85. DOI: 10.14710/ijred.7.2.85-91

Jordan Renewable Energy & Energy Efficiency Law No. 13, (2012).

Ju, X., Xu, C., Liao, Z., Du, X., Wei, G., Wang, Z., & Yang, Y. (2017). A review of concentrated photovoltaic-thermal (CPVT) hybrid solar systems with waste heat recovery (WHR). *Science bulletin*, *62*(20), 1388-1426. DOI: 10.1016/j.scib.2017.10.002

Kumar, R., & Rosen, M. A. (2011). Performance evaluation of a double pass PV/T solar air heater with and without fins. *Applied Thermal Engineering*, *31*(8-9), 1402-1410. DOI: 10.1016/j.applthermaleng.2010.12.037

Lamnatou, C., & Chemisana, D. (2017). Photovoltaic/thermal (PVT) systems: A review with emphasis on environmental issues. *Renewable energy*, *105*, 270-287. DOI: 10.1016/j.renene.2016.12.009

Mansy, E. E., Hetata, A. Y., & Nasr, A. R. (2020). Modeling of water cooled concentrated photovoltaic (CPV) system fed a small campus in Mansoura University–Egypt. *MEJ. Mansoura Engineering Journal*, *43*(1), 7-14. DOI: 10.21608/bfemu.2020.94508

Mojumder, J. C., Chong, W. T., Ong, H. C., & Leong, K. Y. (2016). An experimental investigation on performance analysis of air type photovoltaic thermal collector system integrated with cooling fins design. *Energy and Buildings*, *130*, 272-285. DOI: 10.1016/j.enbuild.2016.08.040

Mustapha, M., Fudholi, A., Yen, C. H., Ruslan, M., & Sopian, K. (2018). Review on energy and exergy analysis of air and water based photovoltaic thermal (PVT) collector. *International Journal of Power Electronics and Drive Systems*, *9*(3), 1367-1373. DOI: 10.11591/ijpeds.v9.i3.pp1367-1373.

Nijmeh, S., Hammad, B., Al-Abed, M., & Bani-Khalid, R. (2020). A Technical and Economic Study of a Photovoltaic-phase Change Material (PV-PCM) System in Jordan. *Jordan Journal of Mechanical & Industrial Engineering*, *14*(4), 371-379.

Odungat, M. M., Simon, S. P., Kumar, K. A., Sundareswaran, K., Nayak, P. S., & Padhy, N. P. (2020). Estimation of system efficiency and utilisation factor of a mirror integrated solar PV system. *IET Renewable Power Generation*, *14*(10), 1677-1687. DOI: 10.1049/iet-rpg.2019.0804

Okorieimoh, C. C., Norton, B., & Conlon, M. (2020). Long-Term durability of solar photovoltaic modules. *Sustainable Ecological Engineering Design*, 317-325. DOI: 10.1007/978-3-030-44381-8_24

Rajput, P., Tiwari, G. N., Sastry, O. S., Bora, B., & Sharma, V. (2016). Degradation of mono-crystalline photovoltaic modules after 22 years of outdoor exposure in the composite climate of India. *Solar Energy*, *135*, 786-795. DOI:10.1016/j.solener.2016.06.047

Rekha, L., Vazhappilly, C. V., & Melvinraj, C. R. (2016). Numerical simulation for solar hybrid photovoltaic thermal air collector. *Procedia Technology*, *24*, 513-522. DOI: 10.1016/j.protcy.2016.05.088

Rizk, J., & Nagarial, M. H. (2009). Impact of reflectors on solar energy systems. *International Journal of Electrical and Electronics Engineering*, 3-9. DOI: 10.5281/zenodo.1057845

Rukman, N., Fudholi, A., Taslim, I., Indrianti, M., Manyoe, I., Lestari, U., & Sopian, K. (2019). Electrical and thermal efficiency of air-based photovoltaic thermal (PVT) systems: An overview. *Indonesian Journal of Electrical Engineering and Computer Science*, *14*(3). DOI: 10.11591/ijeecs.v14.i3.pp1134-1140.

Sarhaddi, F., Farahat, S., Ajam, H., & Behzadmehr, A. (2010). Exergetic performance assessment of a solar photovoltaic thermal (PV/T) air collector. *Energy and Buildings*, *42*(11), 2184-2199. DOI: 10.1016/j.enbuild.2010.07.011

Sarhaddi, F., Farahat, S., Ajam, H., Behzadmehr, A. M. I. N., & Adeli, M. M. (2010). An improved thermal and electrical model for a solar photovoltaic thermal (PV/T) air collector. *Applied energy*, *87*(7),2328-2339. DOI: 10.1016/j.apenergy.2010.01.001

Schwingshackl, C., Petitta, M., Wagner, J. E., Belluardo, G., Moser, D., Castelli, M., ... & Tetzlaff, A. (2013). Wind effect on PV module temperature: Analysis of different techniques for an accurate estimation. *Energy Procedia*, *40*, 77-86. DOI: 10.1016/j.egypro.2013.08.010

Shanks, K., Senthilarasu, S., & Mallick, T. K. (2016). Optics for concentrating photovoltaics: Trends, limits and opportunities for materials and design. *Renewable and Sustainable Energy Reviews*, *60*, 394-407. DOI: 10.1016/j.rser.2016.01.089

Slimani, M. E. A., Amirat, M., Kurucz, I., Bahria, S., Hamidat, A., & Chaouch, W. B. (2017). A detailed thermal-electrical model of three photovoltaic/thermal (PV/T) hybrid air collectors and photovoltaic (PV) module: Comparative study under Algiers climatic conditions. *Energy conversion and management*, *133*, 458-476. DOI: 10.1016/j.enconman.2016.10.066

Suntech. STP285-24/Vd.(2011). Polycrystalline Solar Module. EN-STD-Vd-NO1.01-Rev 2011 ed. China.

Tiwari, A., & Sodha, M. S. (2007). Parametric study of various configurations of hybrid PV/thermal air collector: experimental validation of theoretical model. *Solar Energy Materials and Solar Cells*, *91*(1), 17-28. DOI: 10.1016/j.solmat.2006.06.061

Tiwari, S., Agrawal, S., & Tiwari, G. N. (2018). PVT air collector integrated greenhouse dryers. *Renewable and Sustainable Energy Reviews*, *90*, 142-159. DOI: 10.1016/j.rser.2018.03.043

Umoette, A. T., Ubom, E. A., & Akpan, I. E. (2016). Comparative Analysis of Three NOCT-Based Cell Temperature Models. *Int. J. Syst. Sci. Appl. Math*, *1*(4), 69. DOI: 10.11648/j.ijssam.20160104.16